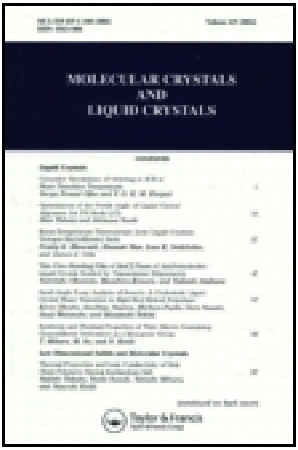

Molecular Crystals and Liquid Crystals Science and Technology. Section A. Molecular Crystals and Liquid Crystals

Publication details, including instructions for authors and subscription information:
http://www.tandfonline.com/loi/gmcl19

Nano-Phase Polymer Dispersed Liquid Crystals

R. Blacker [a] , K. Lewis [a] , I. Mason [a] , I. Sage [a] & C. Webb [a]

[a] Defence Evaluation and Research Agency, St. Andrew's Road, Gt. Malvern, UK

To cite this article: R. Blacker, K. Lewis, I. Mason, I. Sage & C. Webb (1999): Nano-Phase Polymer Dispersed Liquid Crystals, Molecular Crystals and Liquid Crystals Science and Technology. Section A. Molecular Crystals and Liquid Crystals, 329:1, 187-198

To link to this article: http://dx.doi.org/10.1080/10587259908025940

Mol. Cryst. Liq. Cryst., 1999, Vol. 329, pp. 187-198
Reprints available directly from the publisher
Photocopying permitted by license only

Published by license under the
Gordon and Breach Science *Publishers imprint.*
Printed in Malaysia

Nano-Phase Polymer Dispersed Liquid Crystals

R. BLACKER, K. LEWIS, I. MASON, I. SAGE and C. WEBB

Defence Evaluation and Research Agency, St. Andrew's Road, Gt. Malvern, UK

We have studied Polymer Dispersed Liquid Crystal (PDLC) materials based on a recently reported fast reacting formulation. This material consists of extremely small droplets (~ 10 nm in diameter) of liquid crystal within a polymer matrix, we have termed this nano-phase PDLC (n-PDLC). Due to the size of these droplets this material exhibits a non-scattering nature. Instead, this transparent non-scattering material allows voltage control of its effective bulk refractive index. This has many implications, allowing the construction of polarisation insensitive liquid crystal devices. In this work we have designed, fabricated and tested a novel etalon device based on n-PDLC.

Keywords: PDLC; Fabry-Perot

INTRODUCTION

Polymer Dispersed Liquid Crystals (PDLC) are a well known electro-optical material with application as a switchable scatterer of visible wavelength light[1]. These materials can be formed by several techniques. The most common are photopolymerisation induced phase separation (PIPS), thermally induced phase separation (TIPS) and solvent induced phase separation (SIPS)[2,3]. The system chosen for our work was the PIPS process in which a mixture of monomer and liquid crystal is cured causing the liquid crystal to drop out of solution as the monomer polymerises. The thermodynamics of such a binary polymer/solvent system is described by the Flory - Huggins model relating interaction between solvent and polymer to the reduced Gibbs energy of mixing[4].

The characteristics of PDLC are determined by the speed of polymerisation, which establishes the rate of phase separation. Indeed this phase separation rate defines the droplet morphology (size, shape and to some extent number density)[5]. For scattering PDLC, the parameters controlling the formation are directed to yield droplets in the 1 – 2 micron size range whether by SIPS TIPS or PIPS. This is done to maximise scattering whilst maintaining the droplets at a sufficiently large scale to enable low voltage switching to take place.

The process of droplet formation in a PIPS process is quite complex. In the particular case of photopolymerisation we must consider the effect of the liquid crystal on the polymerisation process. The droplet size, shape and density depend upon such factors as total LC content, the rate at which the curing is taking place and the changing solubility of the LC whilst the polymerisation is taking place. There are therefore two competing processes.

i) The rate of nucleation of the LC inclusions and their subsequent growth.

ii) The rate of gelation of the polymer network. By this we mean the rate at which full cross-linking is achieved. At some time during this process, the liquid crystal moieties lose their mobility in the system and droplets can no longer grow since the LC cannot flow through the matrix into the droplets.

Statistical fluctuations of the free energy of the mix its composition define the position of the droplets.

Detailed studies of the kinetics of photopolymerisation have been undertaken in the past. These studies have examined the effects of small amounts of non reacting components in the mix. However, in the present work a large amount of non reacting component is present. Therefore, the effect of LC diffusion in the mixture at the droplet forming stage is more important in setting droplet size. This means that by controlling the time between the LC dropping out of solution and the final cross-linking we control the droplet size.

MATERIALS STUDIED AND CELL FABRICATION

In these studies, the system considered was suggested by work performed to fabricate PDLC Bragg gratings[6]. Dipentaerythritol penta- /hexa- acrylate (DPEPHA) was chosen as the base monomer system with 1-vinyl-2-pyrrolidinone (1V2P) as the chain extender. Both chemicals were obtained from the Sigma-Aldrich chemical company. Their chemical structures are shown below.

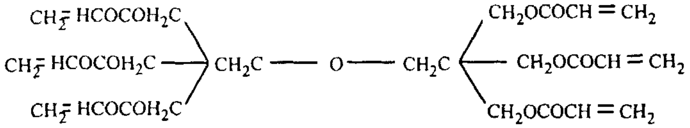

FIGURE 1 DPEPHA

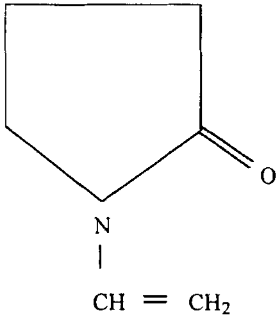

FIGURE 2 1V2P

In order to obtain an uncoloured polymer Darocur 4265 (phenyl – 2 – hydroxy – 2 – propyl ketone) was used as the photoinitiator rather than the more usual Rose Bengal, which exhibits a strong red colouration. Control over the material parameters could be obtained by varying the concentrations of the two components DPEPHA and 1V2P in the monomer mix. Typically 50% - 70% DPEPHA and 50% - 30% 1V2P w/w was used. The higher the percentage of 1V2P, the greater is the elasticity of the polymer.

A high birefringence nematic LC was added to the monomer formulation to give the largest possible electro-optic response. Merck cyanobiphenyl BL36 (Δn = 0.27 @ 589.7nm) was added at a 40% concentration to 60% monomer w/w. To this mixture the Darocur 4265 photoinitiator was added at 5% w/w.

The resulting uncured material had sufficiently low viscosity that both draw bar and cell vacuum filling fabrication methods could be used. The draw bar method was used for assessing the suitability of different formulations and curing processes, the vacuum filling technique was used to fabricate cells for electro-optical testing. Typically, cells were ~12μm thick defined by glass beads within the glue joining the two ITO coated glass plates. . The ITO also gave a very weak etalon effect that could

be modulated by applying an electric field to the cells after curing. In some cells fabrication of a quarter wave mirror stack from SiO_2 and TiO_2 onto each glass/ITO surface enhanced this switchable etalon effect. Cell construction and individual mirror transmissions are shown in figures 3 and 4.

The mirror stack used SiO_2 as the low refractive index and TiO_2 as the high refractive index materials. The cells were cured using a low power, broad band UV source (Teklite ELC400) providing 108 Wcm^{-2} illumination intensity. The mirror stack cells required a high power broad band source (GEW UV source) giving 560 Wcm^{-2}.

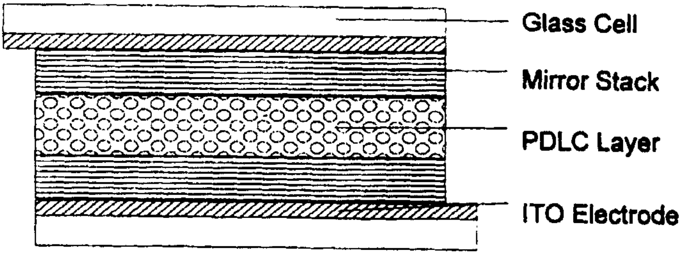

FIGURE 3 Mirror stack cell construction

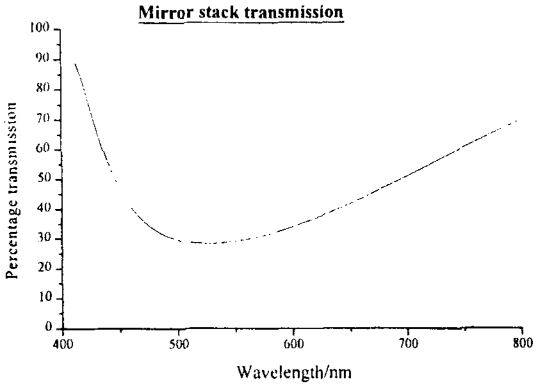

FIGURE 4 Mirror stack transmission

EXPERIMENTAL TECHNIQUES

The spectral response of the etalon devices was assessed using a Perkin-Elmer lambda 9 spectrophotometer as a function of applied fields. Dynamic measurements were taken on a multichannel analyser, which captured a spectrum every 30ms and a laser diode / photodetector system at single wavelength measurements. The measured responses were fitted to the Fabry – Perot etalon equations[7] to calculate the change in refractive index.

$$\frac{I^{(t)}}{I^{(i)}} = \left(1 - \frac{A}{1-R}\right)^2 \frac{1}{1 + F\sin^2\frac{\delta}{2}}$$

Where:

R is the reflectivity of the cavity surfaces

A is the fraction of light absorbed at the cavity surfaces

$$F = \frac{4R}{(1-R)^2}$$

$$\delta = \frac{4\pi}{\lambda_0} hn\cos\theta$$

Where:

λ_0 is the incident wavelength

θ is the angle the light is incident onto the etalon

h is the etalon plate separation

n is the refractive index

This then allowed us to obtain from measurements of the change in refractive index (Δn) an estimate of the effective quadratic electro-optic coefficient Γ of the material itself

$$\overline{\Delta n} = -\frac{1}{2} n_0^3 \Gamma\ E^2$$

Where n_0 is the refractive index changed by the applied electric field E.

The PDLC formed by the draw bar technique was investigated by SEM. The liquid crystal was removed by soxhlet cleansing of the sample[8] before coating a cleaved edge with gold using a field emission system.

RESULTS

Scanning Electron Microscopy

The pure polymer was very difficult to image on the SEM because of the smooth homogeneity of the surface. The LC loaded material showed more surface features and was therefore much easier to image (see figs below).

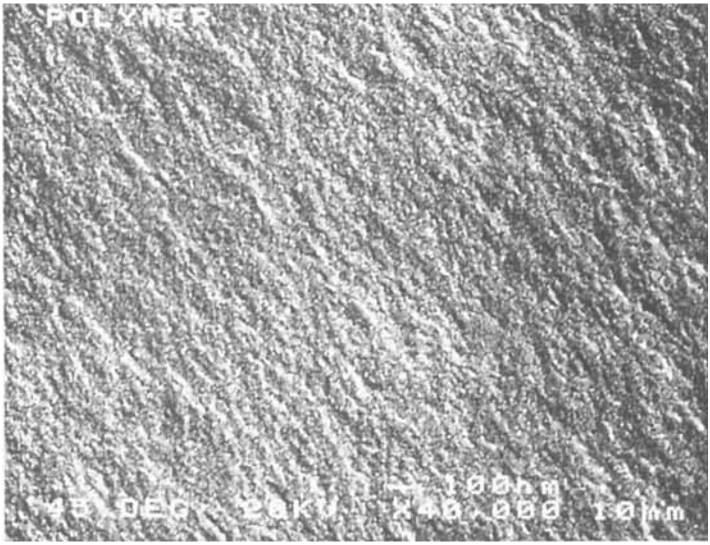

FIGURE 5 SEM of cleaved polymer surface

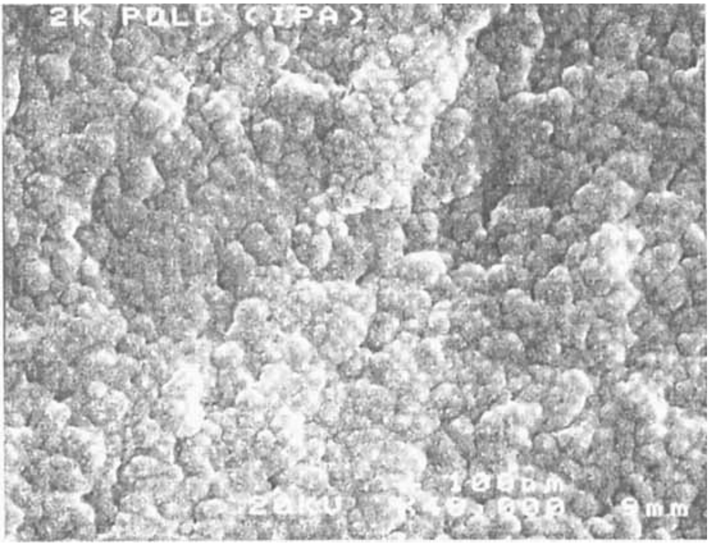

FIGURE 6 Nanodroplet PDLC

The features we observed are reminiscent of the ball type of polymer formations that have been reported in earlier work[9]. This is shown schematically below in fig.7. The spheroid morphology in the SEM is due to the polymer forming a matrix of spheroids with the LC in the inter-spheroid gaps

FIGURE 7 Polymer ball matrix PDLC

The SEM results enabled the amount of LC that had not phase separated to be estimated as 50% of the initial concentration level.

Dynamic Cell Switching

The data from the optical multichannel analyser showed the following changes as a voltage was placed across an 11.6 micron thick cell.

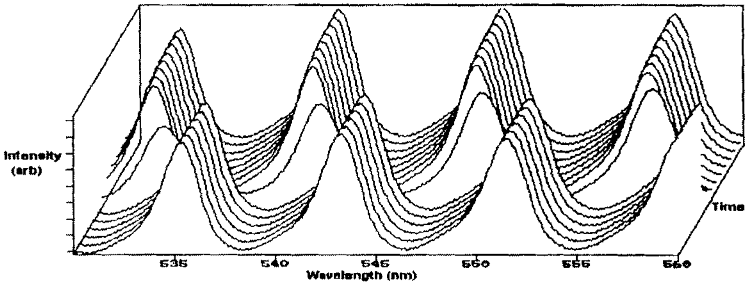

FIGURE 8 Tuning of a BL36 n-PDLC cell – Time runs 0 to 150ms

This waterfall plot (figure 8) has a 30ms time delay between each individual run. At a time of 150ms after the run was initiated a voltage of 300v DC was applied to the cell. A high voltage is required because:-

1) The dielectric mirror stack reduces the effective field across the cell
2) The dielectric mismatch of LC and Polymer leads to the field across each droplet being reduced.

Using the Lever rule[10] with dielectric constants of 3.5 for the polymer and 22.0 for BL36 ($\varepsilon_{\parallel}$) and a 50% inclusion rate as specified above, we obtain that the polymer dielectric constant is raised to 12.75. We can then use the Laplace equation to model dielectric spheres in a differing permittivity host. This led to a model for the 11.6 micron cell at 300 V in which the cell had a field of 24 $V_{\mu}m^{-1}$, but the LC component only sees 3.8 $V_{\mu}m^{-1}$.

Etalon Model

Modelling of an etalon device using the Fabry-Perot equations given earlier to show the same refractive index change gave the result shown in figure 9:

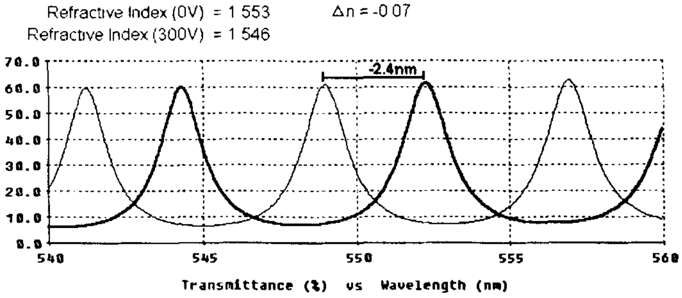

FIGURE 9 Calculated etalon response

The etalon equation gives a refractive index change of 0.07. The figures for the initial refractive index agree with previous work on small droplet systems. The full system gives a Kerr coefficient (R) of 6.5 x 10^{-18} V^2m^{-2}. If we take account of the reduced field effect, we get a figure of 2.6 x 10^{-16} V^2m^{-2}.

The switching voltages are high compared to those normally required for conventional PDLC which are ~20V. The droplet size is however in the range 80nm – 160nm and at this scale length the olefinic tails of the moieties can be enmeshed in the polymeric host. The advantage is that this produces extremely fast relaxation times when the switching voltage is removed. The dynamic measurements made at 670nm with a laser diode have revealed that we can modulate the beam at 16kHz without loss of dynamic range indicating a response time of 62.5$_{\mu}$s.

Other workers in the field have reported similarly formulated systems switching at much lower voltages[11]. However, if one closely observes the SEMs of their gratings as published one sees areas which contain PDLC with larger droplets sizes closer to the size order of standard PDLC. We speculate that these volumes are responding and switching at the lower voltages quoted, but further work would need to be done to confirm this.

CONCLUSIONS

We have investigated a novel form of PDLC. It has been found that we can formulate a PDLC mix that forms nanoscale LC inclusions within a polymer ball matrix. This material exhibits special properties because of the size of these inclusions. Because they are so small, they do not act as strong scattering centres as in standard PDLC. Our Etalon devices demonstrate that this material has a controllable refractive index. The value of the quadratic electro-optic coefficient R is attractive for device exploitation. This value has enabled the demonstration of devices that allow for optical modulation of greater than 50% over ranges of π.

Acknowledgements

The authors thank all of their colleagues at DERA Malvern especially those involved with SEM characterisation.

References

[1] F. Simoni *Advanced Materials in Optics* 243–248 (1995)
[2] K. Takizawa, H Kikuchi, H. Fujikake, Y. Namikawa and K. Tada *Jpn. J. Appl. Phys* **33,** 1346–1351 (1994)
[3] H.S. Kitzerow *Liquid Crystals* **16,** 1, 1–31 (1994)
[3] P. van Konynenburg, S. Marsland and J. McCoy *SPIE,* **823,** 143–150 (1987)
[4] J. Brandrup and E. Immergut *Polymer Handbook 3rd Edition* John Wiley and Sons (1989)
[5] R.L. Sutherland, L.V. Natarajan, V.P. Tondiglia, T.J. Bunning and W.W. Adams *SPIE* **2152,** 303–313 (1994)
[6] T.J. Bunning, L.V. Natarajan, T.P. Tondiglia, R.L. Sutherland *SPIE* **2651,** 44–55 (1996)
[7] M. Born and E. Wolf, *Principles of Optics,* Pergamon Press (1980)
[8] I. Mason, S. Guy, et.al. *Mol. Crys. Liq. Crys. Special Topics* **70** (1994)
[9] R. Yamaguchi and S. Sato, *IEICE Trans. Electron.,* **E78-C,** 1, 106–110 (1995)
[10] J.I. Kroschwitz, *Concise Encyclopaedia of Polymer Science and Engineering,* John Wiley and Sons, 78–82, (1990)
[11] V.P. Tondiglia, L.V. Natarajan, R.L. Sutherland, T.J. Bunning and W.W. Adams, *Optics Letters* **20,** 11, 1325–1327 (1995)